Int. J. Heat Mass Transfer. Vol. 23, pp. 1447–1459

0017-9310/80/1101-1447 $02.00/0

RADIATIVE HEAT TRANSFER IN NONHOMOGENEOUS GASES: A SIMPLIFIED APPROACH

WILLIAM L. GROSSHANDLER
Department of Mechanical Engineering, Washington State University, Pullman, WA 99164, U.S.A.

(*Received* 15 *October* 1979 *and in revised form* 25 *March* 1980)

Abstract — Neither narrow-band nor wide-band models are necessary to accurately model nonhomogeneous effects on radiative heat transfer in high temperature combustion gases. The following article demonstrates the ability of a simplified model, using total transmittance data, to predict the radiance emanating from nonisothermal, variable concentration carbon dioxide and water-vapor mixtures. Computational times using the simplified approach are over two-orders of magnitude less than that required by the Goody statistical narrow-band model with Curtis–Godson approximation, with a sacrifice in accuracy of less than 10%. The total transmittance nonhomogeneous model has been verified for pathlengths between 20 and 200 cm, temperatures between 800 and 1800 K, and CO_2/H_2O ratios between 1/2 and 2.

NOMENCLATURE

a_i, empirical coefficient in emittance equation (3);
C, C_{20}, correction coefficients for transmittance;
C_1, Planck's first radiation constant [W cm^2];
C_2, Planck's second radiation constant [cm K];
d_ω, spectral line space [cm^{-1}];
$\overline{1/d}$, mean strong-line parameter [cm];
e_b, total blackbody emissive power [W cm^{-2}];
$e_{b\omega}$, spectral blackbody emissive power [W/cm^2 cm^{-1}];
I, total radiance or intensity [W cm^{-2} sr^{-1}];
I_ω, spectral radiance or intensity [W cm^{-2} sr^{-1} cm^{-1}];
k_ω, spectral absorption coefficient [cm^{-1}];
l, pathlength [cm];
L, total pathlength [cm];
M, number of homogeneous elements;
n, number of terms in emittance equation (3);
P, pressure [atm];
$\bar{P}$, effective pressure [atm];
R, ideal gas constant [J mole^{-1} K^{-1}];
S, spectral line strength [cm^{-2}];
$\overline{S/d}$, mean line-strength-to-spacing parameter [cm^{-1}];
T, temperature [K];
$\bar{T}$, effective temperature [K];
u, density-pathlength [cm (g cm^{-3})/(g cm^{-3})$_{ref}$];
U, total density-pathlength [cm (g cm^{-3})/(g cm^{-3})$_{ref}$];
X, optical depth;
ε, emittance;
γ_L, spectral line half-width [cm^{-1}];
ρ, density [g cm^{-3}];
σ, Stefan–Boltzmann constant [W cm^{-2} K^{-4}];
τ, τ_ω, total and spectral transmittance;
ω, wave number [cm^{-1}].

Subscripts

0, reference state;
c, carbon dioxide;
CG, Curtis–Godson;
H, homogeneous;
i, index; either c or w in partial pressure;
j, element designation;
w, water vapor;
ω, spectral quantity.

1. INTRODUCTION

PREDICTIVE techniques for radiative heat transfer in fires and combustion systems are often based upon the simplifying assumptions that a single radiative temperature and a single gray absorption coefficient can be ascribed to a specific fuel type, combustion condition and geometry. This has been out of necessity for some real engineering calculations because of the complexity of the other processes which must also be modeled. Although physically unrealistic, the gray gas, isothermal assumption has yielded accurate predictions of heat flux and burning rates in small to moderate size fires [1]. It has also been useful for estimating the total radiative flux in furnace enclosures from entire combustion gas volumes [2].

The gray gas, isothermal assumption can lead to considerable errors in larger scale fires [3]. It cannot be used to predict the distribution of radiant energy along a furnace wall, nor the effect of a cool absorbing layer on the local heat flux. Models with varying degrees of accuracy and complexity have been developed which relax the gray gas, isothermal assumption, a few of which are the statistical narrow-band

model, the exponential wide-band model, and the sum of gray gases zone method. These non-gray models are briefly reviewed, and published experimental data against which to compare them are mentioned. In addition to these established models, a simplified nonhomogeneous model is presented which requires no spectral information. The results of the simplified technique are compared to calculations made using the more complex narrow-band model.

2. BACKGROUND

Consider a cloud of high temperature absorbing/emitting gas, with nonuniform temperature and concentrations, and with nonreflecting cool boundaries. The radiant intensity, I, directed towards the origin along a single line-of-sight through the cloud of pathlength, L, can be found from the solution of the equation of transfer [4], which is

$$I = \int_{\omega=0}^{\infty} \int_0^U k_\omega \frac{e_{b\omega}}{\pi} \exp\left(- \int_0^u k_\omega du' \right) du \, d\omega. \quad (1)$$

k_ω is the spectral absorption coefficient of the gas, and $e_{b\omega}$ is Planck's blackbody distribution function. The integration is performed over all wavenumbers, ω, and along the density-pathlength, given by

$$du = \frac{\rho}{\rho_0} dl = \frac{P}{P_0} \frac{T_0}{T} dl, \qquad U = \int_0^L \frac{\rho(l)}{\rho_0} dl. \quad (2)$$

ρ_0 is the density of the gas at a reference pressure, P_0, and temperature, T_0.

The major complexity of equation (1) is associated with the functional form of the absorption coefficient, which varies in a complex manner with species, wavenumber and temperature. Narrow-band models have been developed to approximate the average behavior of k_ω in a small spectral interval. (See Tien [5] or Tiwari [6] for a general review of the subject.) Within this interval, containing hundreds of individual lines, the mean line strength across the narrow band is found by summing up the contributions from each individual line. Nonisothermal behavior can be accounted for by making use of the Curtis–Godson approximation [7], which appropriately averages the mean line intensity and line spacing over the nonhomogeneous path. Accurate predictions require the narrow band to have a width, in wavenumbers, of about 25 cm^{-1}; the total intensity calculation from a typical combustion gas mixture containing water vapor and carbon dioxide thus requires scanning over about 300 narrow-band regions. The complexity of narrow-band models, and the large amount of computational time which they require, do not make them suitable for most engineering combustion calculations.

Wide-band models reduce the inefficient spectral calculations from 300 down to six or eight. Originally developed by Edwards and Menard [8], the exponential wide-band model treats an entire vibrational band as an array of equally spaced lines, each line arranged within the band to give an exponentially decreasing intensity with increasing distance from the band center. This model is suitable for nonisothermal gases, as verified by measurements in carbon dioxide and water vapor environments by Edwards *et al.* [9]. Other investigators [10, 11] have developed more simplified expressions for the band absorptance, and have used a Curtis–Godson type method to average the band parameters for a nonhomogeneous path. The overlap band at 2.7 μm has been studied by Felske and Tien [12, 13], and their wide-band correlation compared to the experimental measurements of Saido and Giedt [14] in nonisothermal water vapor–carbon dioxide mixtures.

Hottel and Sarofim [15] describe a method for calculating the radiant heat exchange within a furnace using the zoning method, and assuming that the combustion gas is composed of one clear and two gray gases. In general, the emittance, ε, of any homogeneous gas mixture can be written in series form:

$$\varepsilon = \sum_{i=1}^{n} a_i [1 - \exp(-k_i P_i L)]. \quad (3)$$

P_i is the partial pressure of the radiating gas, k_i is an effective absorption coefficient, and a_i is an empirical coefficient found from a curve-fit of total emittance data. Reed [16] extended this approach so that nonisothermal conditions could also be expressed by (3). To do this, he removed the temperature dependence from the absorption coefficient and placed it in the empirical coefficient, a_i.

The simplest approach to nonhomogeneous gas radiation is that originally proposed by Hottel [2]. The radiant heat flux is written in terms of the slope of the total emittance/pressure-pathlength curve in the limit of zero length, multiplied by the total transmittance, τ, averaged along the nonisothermal path. This intensity can be written (see equation 4-64 in [2])

$$I \simeq \int_0^U \tau \left(\frac{d\varepsilon}{du} \right)_{l \to 0} \frac{e_b(l)}{\pi} du. \quad (4)$$

e_b is the blackbody total emissive power, σT^4. This method is particularly convenient because the gradient of total emittance and the transmittance both can be found from the extensive data provided by Hottel in chart form [2].

Leckner [17] used this approach for nonisothermal radiation calculations, and compared his results to detailed spectral calculations. Agreement was good for water vapor at short pathlengths and moderate temperature gradients. Calculations for carbon dioxide were less accurate, especially for the steepest temperature gradients.

Because of the simplicity of this approach and the encouraging results published by Leckner, a model based upon total transmittance data has been developed. The model calculates the radiance and transmittance of a nonisothermal, variable concentration mixture of carbon dioxide, water vapor and air under conditions representative of moderate size, atmospheric combustion. The validity of the simplified

model is determined by comparison to the results obtained from a detailed narrow-band calculation. In the following section, the narrow-band model used as the basis for comparison is put forth; and its accuracy is documented against published experimental results.

3. NARROW-BAND MODEL

The primary infrared bands of interest in high temperature combustion gases are the 1.38, 1.88, 2.7 and 6.3 μm bands of water vapor; and the 2.7 and 4.3 μm bands of carbon dioxide. The Goody statistical model [18] with equal line strengths was chosen to model both of these triatomic molecules, based upon previous work by Ludwig *et al.* [21]. Isolated line broadening is primarily by collisional interactions in combustion systems, so a Lorentz line shape [4] with line half-width γ_L was assumed. The small contribution from Doppler broadening was considered to be additive. With the Goody model, the individual spectral lines are randomly distributed within each narrow-band region. The mean line-strength-to-spacing parameter, $\overline{S/d}$, can be found by summing up the contributions to line strength, S, from each rotational line divided by the distance, d, between adjacent lines. The second narrow-band parameter important in this two-parameter model is the mean inverse line spacing, or the mean strong-line parameter, $\overline{1/d}$. For the carbon dioxide molecule, $\overline{S/d}$ and $\overline{1/d}$ are determined from the modified anharmonic oscillator/rotator model developed by Malkmus [19, 20]. For water vapor, these two parameters have been tabulated as a function of wavenumber and temperature by Ludwig *et al.* [21], based upon extensive experimental measurements [22].

With the mean line-strength-to-spacing parameter and mean strong-line parameter known, the Goody model yields the following expression for the absorption coefficient in a homogeneous gas of pathlength, l

$$k_{\omega,H} = \overline{S/d}\left[1 + \frac{\overline{S/d}\, l\rho/\rho_0}{4\gamma_L\, \overline{1/d}}\right]^{-1/2}. \tag{5}$$

Define the optical depth, X_ω, and the spectral transmittance, τ_ω, along a nonhomogeneous path between 0 and l

$$X_\omega(l) \equiv \int_0^l k_\omega(l')\frac{\rho}{\rho_0}\mathrm{d}l' \tag{6}$$

$$\tau_\omega(l) \equiv e^{-X_\omega(l)}. \tag{7}$$

The problem which occurs in the nonhomogeneous case is to determine the proper value of k_ω to use in (6), since equation (5) is valid only over an isothermal, constant composition path. The Curtis–Godson approximation [7] was developed to deal with this problem, and replaces $\overline{S/d}$ and $\overline{1/d}$ in (5) with suitable averages over the nonhomogeneous path. The absorption coefficient at a location, l, for radiation directed towards the origin, can be written in terms of the Curtis–Godson approximation as

$$k_{\omega,CG}(l) = \overline{S/d}_{CG}\left[1 + \frac{\left(\int_0^l \frac{\rho(l')}{\rho_0}\mathrm{d}l'\right)^2 (\overline{S/d}_{CG})^2}{4\int_0^l \gamma_L\, \overline{1/d}\,(l')\,\overline{S/d}\,(l')\,\rho(l')/\rho_0\,\mathrm{d}l'}\right]^{-1/2} \tag{8}$$

where the Curtis–Godson average of the line-strength-to-spacing parameter is defined by

$$\overline{S/d}_{CG} \equiv \frac{\int_0^l \overline{S/d}\,(l')\,\rho(l')/\rho_0\,\mathrm{d}l'}{\int_0^l \rho(l')/\rho_0\,\mathrm{d}l'}. \tag{8'}$$

For a mixture of carbon dioxide and water vapor, the combined optical depth along a nonhomogeneous path can be found by adding together the contributions to optical depth from each species, determined from (6), at a given wavenumber.

$$X_{\omega,mix}(l) = \int_0^l [k_{\omega,w}(l')P_w(l') + k_{\omega,c}(l')P_c(l')]\frac{T_0}{P_0\,T(l')}\mathrm{d}l' \tag{9}$$

where the subscripts w and c refer to water and carbon dioxide, respectively. Equation (1) can now be written in terms of the optical depth for the mixture.

$$I = \int_{\omega=0}^{\infty}\int_0^L [k_{\omega,w}(l)P_w(l) + k_{\omega,c}(l)P_c(l)]\frac{e_{b\omega}}{\pi} \times \exp[-X_{\omega,mix}(l)]\frac{T_0}{P_0\,T(l)}\mathrm{d}l. \tag{10}$$

Using the definition of transmittance, the total intensity can finally be written as

$$I = -\int_{\omega=0}^{\infty}\int_1^{\tau_\omega(L)} \frac{e_{b\omega}(T,\omega)}{\pi}\mathrm{d}\tau_\omega. \tag{11}$$

A computer code was generated to numerically integrate equation (11) (following the approach suggested by Ludwig *et al.* [21]), with the transmittance calculated along the path of interest from equations (7), (8) and (9). The program, RADCAL, uses the data of Ludwig *et al.* [21] and the models of Malkmus [19, 20] to determine $\overline{S/d}$ and $\overline{1/d}$ for the primary infrared bands of water vapor and carbon dioxide. (Details of the program are available in [23] and [24].) The literature was surveyed for experimental measurements against which to compare the computer predictions. Table 1 is a summary of the nonhomogeneous experimental data reviewed, including the spectral regions measured and the partial pressure-pathlengths covered.

Computer calculations were run on homogeneous and nonhomogeneous mixtures of carbon dioxide and water vapor, as documented in [24]. Figures 1 and 2

Table 1. Nonhomogeneous experimental data from the literature

Experimenters	Spectral region (μm)	Temperature range (°K)	H_2O pressure-pathlength (atm cm)	CO_2 Pressure-pathlength (atm cm)	Comments
Simmons *et al.* [25]	2.7	380–1160	4–53	2–60	Well controlled environment, reliable data
Ludwig *et al.* [22]	2.7	1180–2480	150	0	Temperature, pathlengths and gradients are large
Giedt and Saido [14]	2.7	400–2000	3–30	0.8–18	Covers range of interest
Edwards *et al.* [9]	2.7, 4.3, 15	310–1160	0	1–108	Well controlled
Edwards *et al.* [9]	2.7, 6.3	380–1050	46	0	Well controlled
Grosshandler and Sawyer [26]	1.3–8	800–1800	4	2	Turbulent combustion
Buckius [27]	1.6–5.2	700–1600	0.1–1.9	0.25–2.5	Plastic pool fires
Sato and Kunitomo [31]	total	800–1400	2–4	1–4	Turbulent combustion

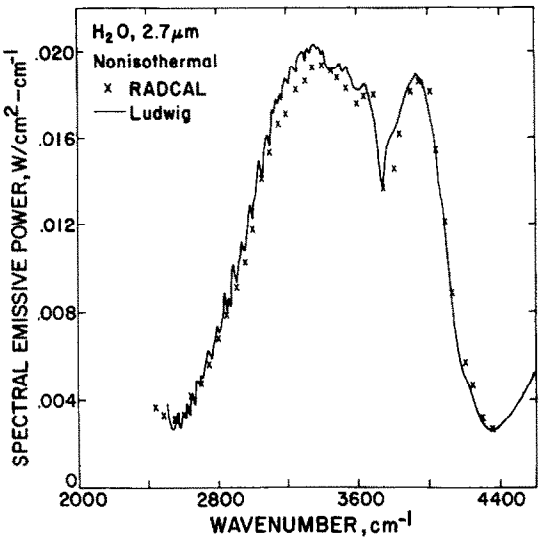

FIG. 1. Spectral emissive power from the 2.7 μm band of nonisothermal H_2O/O_2 mixtures, comparing the results of the narrow-band model to measurements by Ludwig *et al.* [22].

compare the results of RADCAL to two nonhomogeneous measurements of water vapor. The experiment of Ludwig [22], shown in Fig. 1, was on the 2.7 μm band over a long pathlength (150 cm) including high temperatures (2480 K). The spectral emissive power predicted by the narrow-band model agrees with the data across the entire band. Edwards *et al.* [9] measured the spectral absorptance of the 6.3 μm band along a 46 cm nonisothermal path. The essential structure of the measurements is seen, in Fig. 2, to be modeled by the program. The measurements of Simmons *et al.* [25], of the spectral radiance from the 2.7 μm band of nonisothermal carbon dioxide, are compared to RADCAL in Fig. 3, showing excellent agreement. Figure 4 is the spectral absorptance of the 2.7 μm overlap band from a mixture of carbon dioxide and water vapor [25], indicating that the computer calculation also gives a satisfactory result in overlapping nonisothermal mixtures. The final comparison is to the experiment of Grosshandler and Sawyer [26], in which a low resolution spectrum from 1.25 to 8.0 μm, shown in Fig. 5, is modeled with reasonable accuracy.

With the narrow-band model validated against published experimental results, the detailed spectral program was used as the basis for comparison to the simplified total transmittance model.

4. TOTAL TRANSMITTANCE NONHOMOGENEOUS MODEL

In equation (11), the integration over transmittance can be replaced by a summation over M homogeneous elements

$$I_\omega = -\sum_{j=1}^{M} \frac{e_{b\omega}(T_j)}{\pi}(\tau_{\omega_j} - \tau_{\omega_{j-1}}). \qquad (12)$$

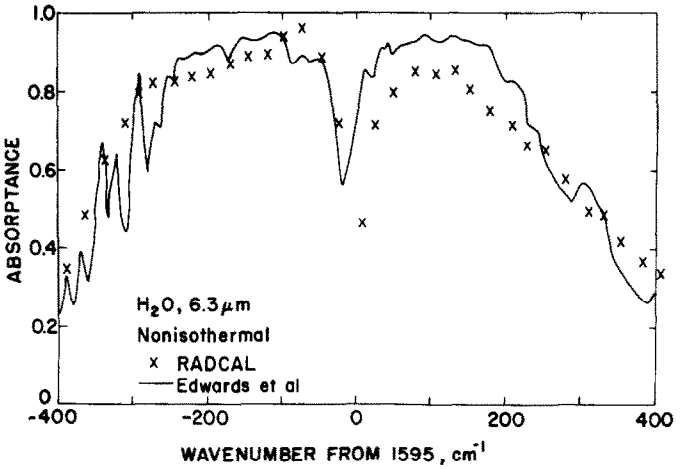

FIG. 2. Spectral absorptance of the 6.3 μm band of nonisothermal H_2O, comparing the results of the narrow-band model to the measurements of Edwards *et al.* [9].

The total intensity is found by integrating over wavenumber.

$$I = -\int_0^\infty \sum_{j=1}^{M} \frac{e_{b\omega}(T_j)}{\pi}(\tau_{\omega_j} - \tau_{\omega_{j-1}})\mathrm{d}\omega$$

$$= \frac{1}{\pi}\sum_{j=1}^{M}\left(\int_0^\infty e_{b\omega}(T_j)\tau_{\omega_{j-1}}\mathrm{d}\omega - \int_0^\infty e_{b\omega}(T_j)\tau_{\omega_j}\mathrm{d}\omega\right). \quad (13)$$

The total transmittance for a homogeneous path is defined [4] in terms of the spectral transmittance, and is given by

$$\tau(T,P,l) \equiv \frac{\int_0^\infty e_{b\omega}(T)\tau_\omega(T,P,l)\mathrm{d}\omega}{\sigma T^4}. \quad (14)$$

Assume that an effective temperature, $\bar{T}$, and an effective pressure of radiating species, $\bar{P}$, exist over a nonhomogeneous path, such that

$$\tau(\bar{T},\bar{P},l) \equiv \frac{\int_0^\infty e_{b\omega}(l)\tau_\omega(l)\mathrm{d}\omega}{\sigma T(l)^4}. \quad (15)$$

Use equation (15) to approximate the integrals in the RHS of equation (13) as

$$\sigma T_j^4 \tau_{j-1}(\bar{T}_{j-1}, \bar{P}_{j-1}, l_{j-1})$$

and

$$\sigma T_j^4 \tau_j(\bar{T}_j, \bar{P}_j, l_j),$$

respectively. Then the radiance becomes

$$I \simeq \frac{\sigma}{\pi}\sum_{j=1}^{M} T_j^4(\tau_{j-1} - \tau_j). \quad (16)$$

In the narrow-band model discussed in Section 3, the total radiance is found from equation (11) by the integration over all wave numbers, after the blackbody function and transmittance are integrated along the nonhomogeneous path. Notice that the approximate equation (16) results from reversing the order of integration. This is effectively what Hottel has done in obtaining equation (4).

A method must be devised to calculate $\bar{T}$ and $\bar{P}$. Leckner [17] used a partial-pressure weighted tem-

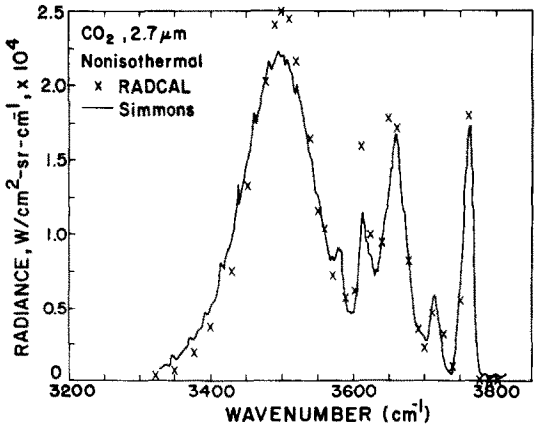

FIG. 3. Spectral radiance from the 2.7 μm band of nonisothermal CO_2, comparing the results of the narrow-band model to the measurements of Simmons *et al.* [25].

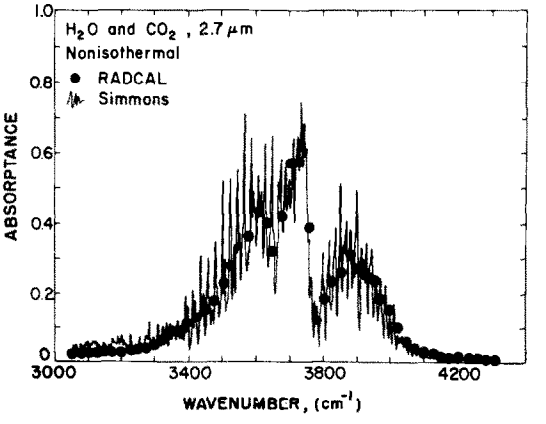

FIG. 4. Spectral radiance from the 2.7 μm overlap band of a nonisothermal mixture of H_2O and CO_2, comparing the results of the narrow-band model to the measurements of Simmons *et al.* [25].

Table 3. Effect of CO_2/H_2O ratio on total transmittance model

	1:2	2:2	2:1
Exact method (RADCAL), $W\,cm^{-2}\,sr^{-1}$	1.739	1.830	1.394
Approximate method (TTNH), $W\,cm^{-2}\,sr^{-1}$	1.478	1.541	1.150
Deviation, %	−15.0	−15.8	−17.5

Note: The temperature profile is as in configuration A..

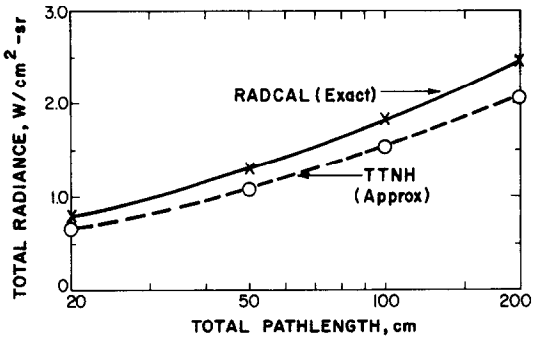

FIG. 8. The effect of total pathlength on the radiance from a CO_2/H_2O/air mixture with temperature profile similar to configuration A. The simplified model, TTNH, is compared to the narrow-band model, RADCAL.

terms of the total transmittance. This is exact only if we can write

$$e_b(T_j)\tau(\bar{T}_{j-1}) = \int_0^\infty e_{b\omega}(T_j)\tau_{\omega_{j-1}}(\bar{T}_{j-1}, \bar{P}_{j-1}, l_{j-1})\mathrm{d}\omega$$

and

$$e_b(T_j)\tau(\bar{T}_j) = \int_0^\infty e_{b\omega}(T_j)\tau_{\omega_j}(\bar{T}_j, \bar{P}_j, l_j)\mathrm{d}\omega.$$

Or, in general (since $T_j \neq \bar{T}_j$)

$$e_b(T_2)\tau(T_1) = \int_0^\infty e_{b\omega}(T_2)\tau_\omega(T_1)\mathrm{d}\omega. \qquad (19)$$

Equation (19) is exact for four conditions: the transmittance is gray, the spectral transmittance is not a function of temperature, T_1 equals T_2, or T_1 and T_2 differ in such a way that

$$e_{b_\omega}(T_2) = \frac{e_b(T_2)}{e_b(T_1)} e_{b_\omega}(T_1). \qquad (20)$$

Investigating this last condition by approximating the blackbody function with Wien's distribution [4], equation (20) implies that

$$\frac{2\pi C_1\omega^3}{\exp(C_2\omega/T_2)} = \frac{\sigma T_2^4}{\sigma T_1^4}\frac{2\pi C_1\omega^3}{\exp(C_2\omega/T_1)}$$

where C_1 and C_2 are Planck's first and second radiation constants. This reduces to the requirement that

$$T_2^4\exp(C_2\omega/T_2) = T_1^4\exp(C_2\omega/T_1). \qquad (21)$$

At $\omega = 3300\,cm^{-1}$, the above expression is approximately constant for temperatures between 1000 and 2000 K; however, at $\omega = 2000\,cm^{-1}$, the variation with temperature is by almost a factor of four, and it becomes two orders of magnitude at $10{,}000\,cm^{-1}$.

Since equation (19) is inexact for a nonisothermal real gas, define a correction coefficient, C, such that

$$C \equiv \frac{\int_0^\infty e_{b_\omega}(T_2)\tau_\omega(T_1)\mathrm{d}\omega}{e_b(T_2)\tau(T_1)}. \qquad (22)$$

The correction factor can be evaluated using the subroutines in RADCAL (see [24])]. This has been done for temperatures between 800 and 1800 K and for temperature ratios, T_1/T_2, between 0.4 and 2.4. The combined water vapor/carbon dioxide pressure-pathlength was varied between 2.0 and 40 atm cm, and the CO_2/H_2O ratio was set equal to 1:2, 1:1, and 2:1. C is plotted in Fig. 9 as a function of T_1/T_2 with the combined pressure pathlength ($P_w l + P_c l$) as a parameter. The error bars indicate the scatter caused by the different temperatures and pressure ratios used.

The correction coefficient for a combined pressure-pathlength of 20 atm cm can be fit to a polynomial of the form

$$C_{20} = 1.4109 - 0.7713\left(\frac{T_1}{T_2}\right) + 0.5516\left(\frac{T_1}{T_2}\right)^2 - 0.2268\left(\frac{T_1}{T_2}\right)^3 + 0.03563\left(\frac{T_1}{T_2}\right)^4. \qquad (23)$$

The value for C at other pressure-pathlengths between 2 and 40 atm cm can then be found from

$$\ln C = [(P_c l + P_w l)/20]^{0.35}\ln C_{20}. \qquad (24)$$

The exponent varies somewhat with temperature, but a value of 0.35 gives a good fit, on the average. *Equations (23) and (24) should be used with caution outside of the temperature and pressure regimes for which they were designed.*

The approximate calculations discussed earlier were repeated with equation (16) modified to include C; that is

$$I \simeq \frac{\sigma}{\pi}\sum_{j=1}^{M} T_j^4[C(\bar{T}_{j-1}/T_j, \bar{P}_{j-1}l_{j-1})\tau_{j-1} - C(\bar{T}_j/T_j, \bar{P}_j l_j)\tau_j]. \qquad (25)$$

Almost without exception, the approximate calculations improved significantly, yielding agreement within 6% for many of the cases. A comparison

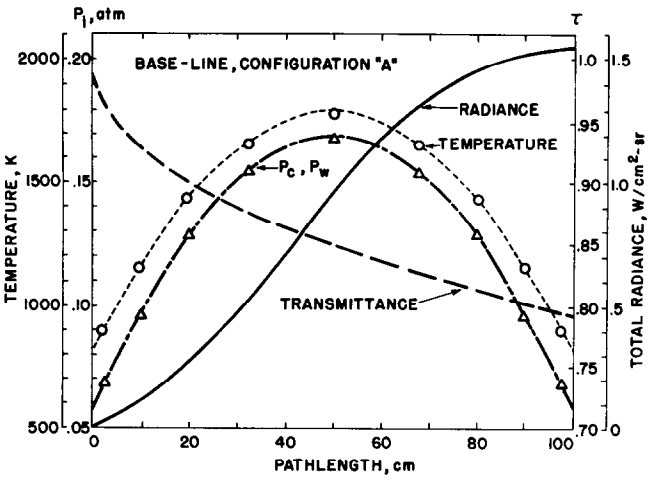

FIG. 6. Temperature and partial pressure profiles in base-line configuration. Symbols indicate location of the assumed homogeneous path elements. Also plotted are the transmittance and radiance, viewed from the origin, as successive elements are added to the gas cloud.

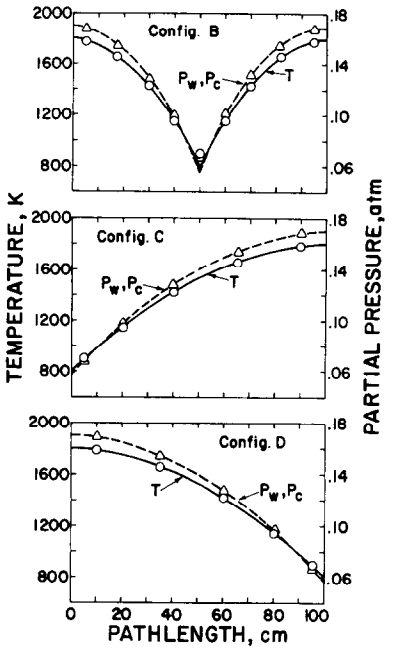

FIG. 7. Temperature and partial pressure profiles for configurations B, C and D.

slightly for the longest pathlength.

For a particular fuel, the local concentration of CO_2 and H_2O will change throughout the combustion zone but the CO_2/H_2O ratio will remain relatively near the thermodynamic equilibrium value. The stoichiometric partial pressure for CO_2 in polystyrene, plexiglass (PMMA), and Delrin fires is between about 0.16 and 0.17 atm, and the CO_2/H_2O ratio varies between 2:1 and 1:1 [27]. In methane combustion, the water vapor is about twice the carbon dioxide concentration. The effect of CO_2/H_2O variations between 1:2 and 2:1 was investigated using the base-line temperature profile. In all cases, the maximum partial-pressure was equal to 0.17 atm. From Table 3, the effect on total radiance is evident, but the deviation between the approximate and exact calculations increases only 2.5% between the worst and best case.

The maximum error in the TTNH model for all of the numerical experiments performed was 19%, which may be of sufficient accuracy if the gaseous radiation contributes less than half to the total heat flux from the flame. The underprediction was greatest for those cases involving positive temperature gradients, suggesting that the calculations may be improved if the transmittance is not only related to the effective temperature, but also to the sense of the temperature gradient. This can be done by re-examining the approximations made in the TTNH model.

In going from equation (13) to equation (16), it was assumed that the integrals could be approximated in

Table 2. Effect of configuration* on total transmittance model

	A	B	C	D
Exact method (RADCAL), $W cm^{-2} sr^{-1}$	1.830	2.333	1.637	2.497
Approximate method (TTNH), $W cm^{-2} sr^{-1}$	1.541	2.327	1.325	2.614
Deviation, %	−16	−0.3	−19	+4.7

* Refer to Figs. 6 and 7 for description of configurations.

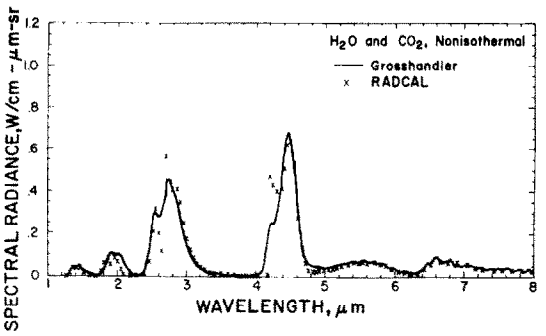

FIG. 5. Spectral radiance from a methanol furnace, comparing the results of the narrow-band model to the measurements of Grosshandler [23].

perature average for $\bar{T}$ and a reduced mass-pathlength equal to

$$\int_0^l 273/T(l')P\,dl'.$$

Rather than partial-pressure, a more appropriate weighting function for temperature is the total number of radiating molecules along the path, i.e., the concentration, or $(P_{cj} + P_{wj})/RT_j$ (c and w indicate carbon dioxide and water). Therefore, define $\bar{T}_j$ as

$$\bar{T}_j \equiv \frac{\int_0^{l_j} T(l)\{[P_c(l) + P_w(l)]/RT(l)\}\,dl}{\int_0^{l_j} \{[P_c(l) + P_w(l)]/RT(l)\}\,dl}$$

or

$$\bar{T}_j \equiv \int_0^{l_j} [P_w(l) + P_c(l)]\,dl \Big/ \int_0^{l_j} \{[P_w(l) + P_c(l)]/T(l)\}\,dl. \quad (17)$$

A reasonable weighting function for the effective partial pressure, $\bar{P}_j$, is the number of molecules of the ith species along the absorbing path.

$$\bar{P}_{ij} \equiv \frac{\int_0^{l_j} P_i(l)[P_i(l)/RT(l)]\,dl}{\int_0^{l_j} [P_i(l)/RT(l)]\,dl}.$$

Therefore,

$$\bar{P}_{cj} \equiv \frac{\int_0^{l_j} [P_c(l)]^2/T(l)\,dl}{\int_0^{l_j} P_c(l)/T(l)\,dl},$$

$$\bar{P}_{wj} \equiv \frac{\int_0^{l_j} [P_w(l)]^2/T(l)\,dl}{\int_0^{l_j} P_w(l)/T(l)\,dl}. \quad (16)$$

The definitions of effective temperature and effective partial pressures, together with the transmittance approximation necessary to go from equations (13)–(16), make up the total transmittance nonhomogeneous model (TTNH). The model reduces to the exact solution if the gases are truly gray or if the path is isothermal. Its validity for other conditions important in combustion research will be demonstrated in the following discussion.

The advantage of the total transmittance model lies in the elimination of all spectral calculations, with the use, instead, of the available isothermal total emittance data from sources such as Hottel's charts [2]. However, because there are limited measurements of total radiance in nonhomogeneous gas mixtures, it is not possible to validate the simplified model by comparison with experiment. Nevertheless, the TTNH model can be verified by comparison against the 'exact' narrow-band model using RADCAL. To eliminate discrepancies due to different data bases, total transmittance data analogous to what would be found in Hottel's charts were generated using RADCAL. Using this data, a numerical program was written to calculate the radiance in nonhomogeneous systems from equations (15)–(18). (A listing of the program is given in [24].)

A base-line condition was chosen to approximate the temperature and partial-pressure distributions one might find parallel to the surface of a 1 m Delrin pool fire. Parabolic profiles were assumed for both temperature and CO_2/H_2O partial-pressures, ranging from 800 K and 0.06 atm at the edge to 1800 K and 0.17 atm at the centerline. The radiance leaving this fire was calculated by the narrow-band model to be equal to 1.830 W/cm² sr, whereas the approximate method using the TTNH model yielded a radiance of 1.541 W cm² sr. Figure 6 is a plot of the transmittance and radiance calculated for this flame as additional elements were added to the line of sight. The temperature profile and partial pressures are also plotted in Fig. 6, with the circles and triangles indicating the center point of the nine homogeneous elements. Those elements furthest from the origin contribute the least to transmittance and total radiance, as indicated by the reduced slope of the curves.

Using the same average pressures and temperature and a constant total length of 100 cm, the base-line profile was rearranged into the three additional configurations drawn in Fig. 7. The results of the exact and approximate radiance calculations are summarized in Table 2 for all four configurations. The approximate method is seen to be most accurate when a hot radiating layer is closest to the origin. The agreement is less satisfactory when a cold absorbing layer exists at the outer region of the cloud.

With the profile maintained similar to configuration A, the total path was varied an order-of-magnitude to determine the effect on the accuracy of the prediction. The results are shown in Fig. 8. The approximate method consistently underpredicts the exact calculation, although the percent deviation decreases

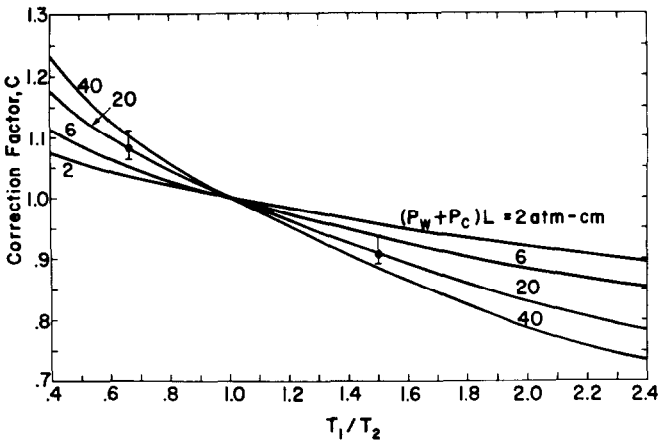

FIG. 9. Transmittance correction factor as a function of temperature ratio and combined pressure-pathlength. Valid for CO_2/H_2O ratios between 1:2 and 2:1 and temperatures between 800 and 1800 K.

showing the improvement in the corrected TTNH model is summarized in Table 4. The last two entries in the table provide a severe test of the correction coefficient. The CO_2/H_2O partial-pressure ratio was allowed to vary between 1:2 and 2:1 along the line-of-sight. In one case the calculation improved to within 2% of the exact solution, while in the other case, the error increased 1.3% while using the correction coefficient. The type of pressure-ratio variation used in these last two calculations is outside the condition for which the curve fit for C can be expected to be optimum; however, this is also atypical of many combustion systems.

Total emittance data for homogeneous mixtures of CO_2, H_2O, and soot have been recently compiled by Modak in a convenient computer program called ABSORB [28]. The total transmittance determined from RADCAL reproduces the transmittance from ABSORB within about $\pm 5\%$, so the characteristics of nonhomogeneous flames should be qualitatively predicted from both data bases. Radiance calculations with the TTNH model using both RADCAL and ABSORB for the data, have been made for three additional configurations typical of combustion environments:

Configuration E — line-of-sight along the vertical centerline from the surface of an 80 cm PMMA pool fire.

Configuration F — line-of-sight outward from an 80 cm PMMA pool fire, located close to the horizontal fuel surface.

Configuration G — line-of-sight outward through the center, and perpendicular to the axis, of a 20 cm methanol furnace.

The temperature and composition profiles for these configurations are shown in Figs. 10, 12 and 14. Soot is included in the first two to simulate pyrolysis products as well as particulates. The values chosen in E and F were best estimates based upon recent measurements by Modak [29] and Markstein [30]. Configuration G was measured experimentally by Grosshandler [26]. (In this measurement, the total radiance was corrected for reflected energy as well as spectrometer cutoff above 8 μm.) Figures 11 and 13 show the distribution of radiance and transmittance within the simulated

Table 4. Comparison between corrected and uncorrected TTNH model

Configuration	Pathlength (cm)	CO_2/H_2O (atm/atm)	Exact radiance ($W\,cm^{-2}\,sr^{-1}$)	Percent deviation from exact radiance (uncorrected)	(corrected)
A	100	1:1	1.830	−15.8	+5.4
B	100	1:1	2.333	−0.3	−1.7
C	100	1:1	1.637	−19.1	+5.7
D	100	1:1	2.497	+4.7	−1.5
A	20	1:1	0.805	−17.5	+10.1
A	50	1:1	1.295	−16.8	+6.8
A	200	1:1	2.443	−16.1	+3.8
A	100	1:2	1.739	−15.0	+5.2
A	100	2:1	1.394	−17.5	+7.6
C	100	variable	1.320	−12.9	+13.7
D	100	variable	2.082	+6.3	−1.2

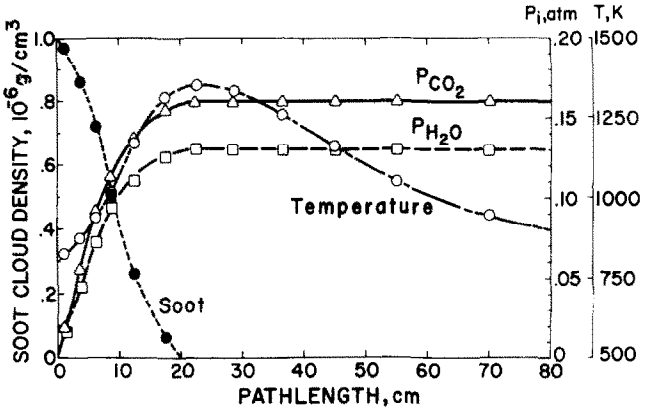

FIG. 10. Composition and temperature profiles simulating the centerline of a PMMA pool fire, config. E.

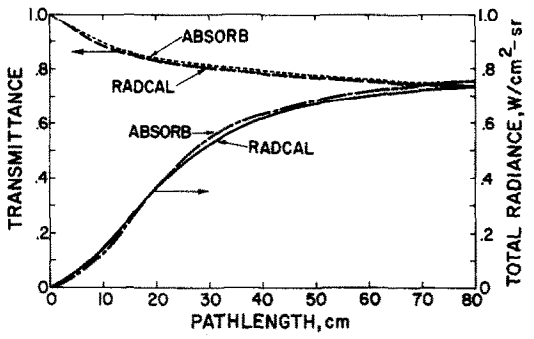

FIG. 11. Transmittance and radiance to fuel surface of simulated PMMA pool fire (see Fig. 10). Calculation is made with the corrected TTNH model, using either ABSORB or RADCAL to compute total radiation properties.

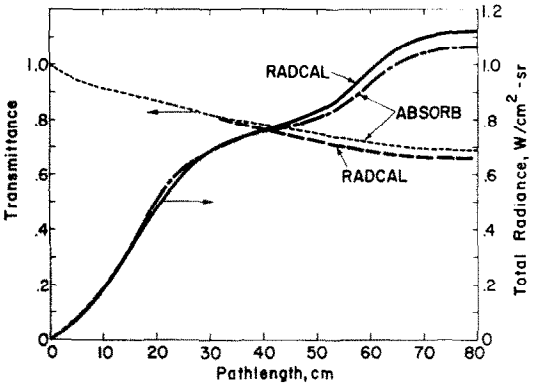

FIG. 13. Transmittance and radiance emanating from a simulated PMMA pool fire (see Fig. 12). Calculation is made with the corrected TTNH model, using either ABSORB or RADCAL to compute radiation properties.

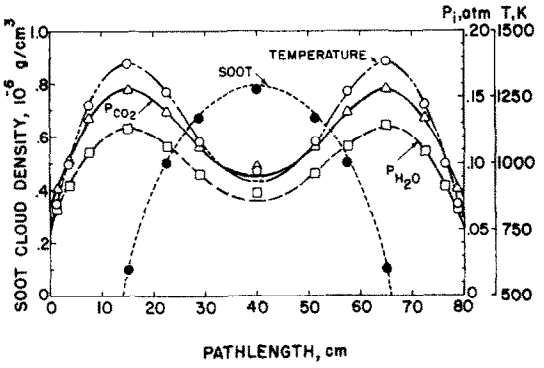

FIG. 12. Composition and temperature profiles simulating a horizontal line-of-sight through a PMMA pool fire, config. F.

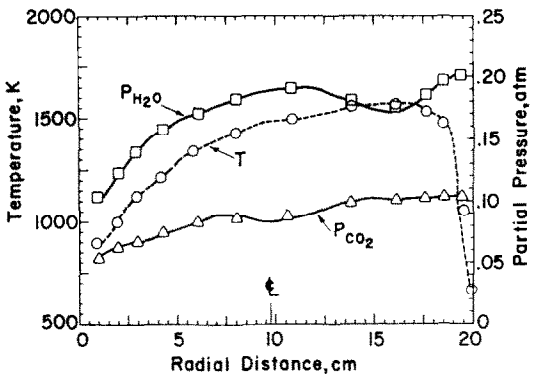

FIG. 14. Composition and temperature profiles measured within a methanol furnace [23], config. G.

PMMA fires, and compare the results of the corrected TTNH model using ABSORB to those using RADCAL as the data base. Further comparison is provided by Table 5. All trends predicted by TTNH using RADCAL data are predicted similarly using ABSORB data, and the degree of agreement speaks well for the validity of the simplified model. The correction coefficient improved both sets of calculations in a similar manner. The ability to predict the radiance in configuration G within 7% of the measured value is strong evidence of the accuracy of the corrected TTNH model in a real combustion environment.

Since the purpose of the simplified radiation model is to reduce computational time, it is interesting to compare the processing time required to that of the narrow-band model. Both the narrow-band model

Table 5. Results of the TTNH model comparing between total transmittance data computed from RADCAL and from ABSORB

Configuration	Exact* radiance ($W\,cm^{-2}\,sr^{-1}$)	Percent deviation of TTNH from exact calculation using ABSORB	(corrected)	RADCAL	(corrected)
A	1.830	−18.7	(+2.2)	−15.8	(+5.4)
B	2.333	−2.9	(−0.2)	−0.3	(−1.7)
C	1.637	−22	(+2.6)	−19.1	(+5.7)
D	2.497	+5.8	(−0.3)	+4.7	(−1.5)
E	0.7016	−2.1	(+7.3)	−5.0	(+4.3)
F	1.086	−10.1	(−1.8)	−4.8	(+3.4)
G	0.68	−12.1	(+6.9)	—	—

*In configurations A–F, exact calculation is with the narrow-band model. In configuration G, exact implies the measured value.

and TTNH (using ABSORB with the correction coefficient) were run with nonhomogeneous profiles of CO_2 and H_2O. With compilation and internal linkage times subtracted from the total computer processing time, the average time for execution was 0.023 s per element for the simplified model, as compared to 7.8 s per element for the narrow-band model.

To appreciate the magnitude of these savings, consider the problem of a nonhomogeneous pool fire in which an accurate estimate of the heat flux to the fuel surface is required. Let the fire volume be divided into four solid-angle regions above a small area on the base, such that a path made up of ten homogeneous elements can be constructed in a radial direction away from the area. If the base is made up of ten such areas, the complete heat flux distribution across the surface would require $4 \times 10 \times 10 = 400$ calculations. Using TTNH this could be completed in 9.3 s of execution time (which must be added to 5 s of compilation, time or about 14 s total). The same computation with the narrow-band model would consume about 52 min, with an expected increase in accuracy of less than 10%.

Although no direct comparison was made to computations using a wide-band model, it is estimated that the simplified method would be from five to ten times faster. The accuracy of the wide-band approach in predicting the total intensity from nonhomogeneous combustion gases would also be expected to be within 10%.

5. CONCLUSIONS

The thermal radiation in nonisothermal, variable concentration combustion has been investigated. The spectral nature of the combustion products and a narrow-band statistical model for carbon dioxide and water vapor have been reviewed. Spectral calculations of radiance and transmittance using the narrow-band model and the Curtis–Godson approximation have been shown to agree with nonisothermal measurements of other investigators.

A simplified method has been presented to calculate the total radiance in nonhomogeneous combustion gases. For conditions similar to non-sooting flames, the total transmittance nonhomogeneous model (TTNH) is in reasonable agreement with the narrow-band model. The accuracy is improved significantly with the introduction of a correction factor to the total transmittance to account for relative differences in temperature along the line-of-sight.

The following conclusions are evident:

(1) The program RADCAL successfully models the spectral nature of the vibrational-rotational bands of carbon dioxide (2.7 and 4.3 μm) and water vapor (1.38, 1.88, 2.7 and 6.3 μm). For temperatures above 800 K, the results can be used as the basis for comparison against simplified gray models in both homogeneous and nonhomogeneous environments.

(2) The simplified total transmittance model (TTNH) can be used to predict the radiance from nonisothermal, variable concentration CO_2/H_2O mixtures. Accuracy can be expected within 20%, while computational time is reduced over two orders-of-magnitude below that for the narrow-band model.

(3) By using a correction factor in the calculation of total transmittance, the accuracy of the TTNH model can be significantly increased. Within the limits of the model (2 to 40 atm cm, P_c/P_w between 0.5 and 2.0, and temperatures from 800 to 1800 K), agreement within 8% can be obtained for most cases.

(4) Neither narrow-band nor wide-band models are needed to obtain sufficiently accurate estimates of radiant heat transfer from and within nonhomogeneous mixtures of CO_2 and H_2O under conditions typical of combustion systems.

Work is continuing with the simplified nonhomogeneous model to incorporate soot radiation in an analytical manner. Indications are that this will improve the accuracy of the model. Experiments measuring the total radiance and absorptance in well characterized, nonisothermal mixtures of hydrocarbon and combustion gases are planned to test the applicability of the TTNH model to more complex combustion environments.

Acknowledgements — This work was accomplished at Factory Mutual Research Corporation under the visiting summer scientist program. The success of the effort is due to the many useful discussions held with Dr. Ashok Modak, and the

inspiration provided by Dr. John de Ris. The assistance given by the entire Basic Research staff is also acknowledged. Partial support was provided by the Thermal Energy Laboratory of Washington State University, Pullman, Washington.

REFERENCES

1. A. T. Modak, Thermal radiation from pool fires, *Combust. Flame* **29,** 177–192 (1977).
2. H. C. Hottel, in *Heat Transmission*, W. H. McAdams (editor) 3rd edition, McGraw-Hill, New York (1954).
3. J. de Ris, Fire radiation — a review, *Seventeenth Symposium (International) on Combustion*, p. 1003, The Combustion Institute, Pittsburgh (1979).
4. R. Siegel and J. Howell, *Thermal Radiation Heat Transfer*, McGraw-Hill, New York (1972).
5. C. L. Tien, Thermal radiation properties of gases, *Adv. Heat Transf.* **5,** 253–324 (1968).
6. S. N. Tiwari, Models for infrared atmospheric radiation, *Adv. Geophys.* **20,** 1–85 (1978).
7. R. M. Goody, *Atmospheric Radiation I, Theoretical Basis*, Clarendon Press, Oxford (1964).
8. D. K. Edwards and W. A. Menard, Comparison of methods for correlation of total band absorption, *Appl. Optics* **3,** 621–625 (1964).
9. D. K. Edwards, L. K. Glassen, W. S. Hauser and J. S. Tuchscher, Radiation heat transfer in nonisothermal nongray cases, *J. Heat Transfer* **86C,** 219–229 (1967).
10. S. H. Chan and C. L. Tien, Infrared radiative heat transfer in nongray nonisothermal cases, *Int. J. Heat Mass Transfer* **14,** 19–26 (1971).
11. R. D. Cess and L. S. Wang, A band absorptance formulation for nonisothermal gaseous radiation, *Int. J. Heat Mass Transfer* **13,** 547–555 (1970).
12. J. D. Felske and C. L. Tien, Infrared radiation from nonhomogeneous gas mixtures having overlapping bands, *J. Quantve Spectros. Radiat. Transf.* **14,** 35 (1974).
13. J. D. Felske and C. L. Tien, Wide band characterization of total band absorption of overlapping infrared gas bands, *Combust. Sci. Technol.* **11,** 111–117 (1975).
14. K. Saido and W. H. Giedt, Spectral absorption of water vapor and carbon dioxide mixtures in the 2.7 μm band, *J. Heat Transfer* **99C,** 53–59 (1977).
15. H. C. Hottel and A. F. Sarofim, *Radiative Heat Transfer*, McGraw-Hill, New York (1967).
16. D. W. Reed, Radiative heat transfer in real nonisothermal gases, D.D.Sc. Dissertation, M.I.T. (1976).
17. B. Leckner, Some elements of radiative heat transfer calculations in flames and gases, *Archiwum Procesów Spalania* **4,** 387–398 (1973).
18. R. M. Goody, *Q. Jl R. Met. Soc.* **78,** 165 (1952).
19. W. Malkmus, Infrared emissivity of carbon dioxide (2.7 μm band), General Dynamics/Astronautics AE63-0047 (1963).
20. W. Malkmus, Infrared emissivity of carbon dioxide (4.3 μm band), *J. Opt. Soc. Am.* **53,** 951–961 (1963).
21. C. B. Ludwig, W. Malkmus, J. E. Reardon and J. A. Thompson, *Handbook of Infrared Radiation from Combustion Gases*, NASA SP-3080 (1973).
22. NASA CR-61233, Study on exhaust plume radiation predictions, *Gen. Dynamics* (1968).
23. W. L. Grosshandler, A study of a model furnace burning methanol and a methanol/coal slurry, Ph.D. Dissertation, University of California, Berkeley (1977).
24. W. L. Grosshandler, Radiation in nonhomogeneous fires, FMRC J.I. OAOE6 · BU-4, RC 79-BT-9, Factory Mutual Research, Norwood, MA (1979).
25. F. S. Simmons, H. Y. Yamada and C. B. Arnold, Measurement of temperature profiles in hot gases by emission–absorption spectroscopy, NASA CR-72491 (1969).
26. W. L. Grosshandler and R. F. Sawyer, Radiation from a methanol furnace, *J. Heat Transfer* **100,** 247–252 (1978).
27. R. O. Buckius, Infrared radiation from a gaseous particulate medium, Ph.D. Dissertation, University of California, Berkeley (1975).
28. A. T. Modak, Radiation from products of combustion, *Fire Res.* **1,** 339–361 (1979).
29. A. T. Modak, The burning of large pool fires, Western States Section, The Combustion Institute, Berkeley, CA (1979).
30. G. H. Markstein, Measurement of the soot absorption coefficient in fires by a fiber optic probe, Eastern Section, The Combustion Institute, Atlanta (1979).
31. T. Sato and T. Kunimoto, Experimental study on luminous flame, *Mem. Fac. Engng, Kyoto Univ.* **31,** *Part I*, pp. 46–49 (1969).

TRANSFERT DE CHALEUR PAR RAYONNEMENT DANS LES GAZ NON HOMOGENES: UNE APPROCHE SIMPLIFIEE

Résumé—Les modèles à bandes étroites ou à larges bandes ne sont pas nécessaires pour représenter les effets de la non homogénéité sur le rayonnement des gaz de combustion à haute température. L'article suivant montre la capacité d'un modèle simplifié utilisant les données de transmittance totale, pour prévoir le rayonnement du gaz carbonique et de la vapeur d'eau en mélange non isotherme et à concentration variable. Les temps de calcul de cette approche simplifiée sont deux fois moindres que ceux relatifs au modèle statistique à bandes étroites de Goody avec l'approximation de Curtis–Godson, avec un abandon de precision inférieur à 10%. La transmittance totale du modèle non homogène a été vérifiée pour des longueurs de parcours entre 20 et 200 cm, des températures entre 800 et 1800 K et des rapports CO_2/H_2O entre 1/2 et 2.

WÄRMEÜBERGANG DURCH STRAHLUNG IN INHOMOGENEN GASEN: EINE VEREINFACHTE NÄHERUNG

Zusammenfassung—Um den Einfluß von Inhomogenitäten auf den Wärmeübergang durch Strahlung in Verbrennungsgasen hoher Temperatur genau zu beschreiben, sind weder Schmal- noch Breitbandmodelle notwendig. Der folgende Artikel beschreibt die Anwendbarkeit eines vereinfachten Modells, bei dem die gesamten Transmissionsdaten benutzt werden, um die von nichtisothermen Mischungen aus Kohlendioxid und Wasserdampf verschiedener Konzentration ausgehende Strahlung zu beschreiben. Die Rechenzeiten bei Verwendung der vereinfachten Näherung sind zweimal geringer als die Zeiten, die bei dem statistischen Schmalband-Modell von Goody mit Curtis–Godson–Näherung benötigt werden. Die Genauigkeitseinbuße beträgt weniger als 10%. Das inhomogene Modell der gesamten Transmission wurde für Weglängen zwischen 20 und 200 cm, Temperaturen zwischen 800 und 1800 K und CO_2/H_2O-Verhältnisse zwischen 1/2 und 2 verifiziert.

ЛУЧИСТЫЙ ТЕПЛОПЕРЕНОС В НЕОДНОРОДНЫХ ГАЗАХ. УПРОЩЕННЫЙ ПОДХОД

Аннотация — Точный расчет влияния неоднородности среды на лучистый теплоперенос в газообразных продуктах сгорания при высоких температурах можно производить, не прибегая к широкополосным и узкополосным зонным моделям. В статье предлагается упрощенная модель, с помощью которой на основе данных о полной пропускательной способности можно рассчитать величину лучистого потока, излучаемого неизотермической смесью двуокиси углерода с водяным паром с переменной концентрацией. Модель позволяет сократить более чем на два порядка время расчета по сравнению со статистической зонной моделью Гуди, в которой используется аппроксимация Кертиса–Годсона, за счет уменьшения точности расчета менее чем на 10%. Справедливость предложенной модели проверена в диапазоне длин волн от 20 до 200 см, температур от 800 до 1800 К для соотношений CO_2/H_2O между 1/2 и 2.